Photodiagnosis and Photodynamic Therapy 23 (2018) 261–269

Contents lists available at ScienceDirect

Photodiagnosis and Photodynamic Therapy

journal homepage: www.elsevier.com/locate/pdpdt

Silica nanoparticles embedded with water insoluble phthalocyanines for the photoinactivation of microorganisms

Estefania Baigorria[1], Eugenia Reynoso[1], M. Gabriela Alvarez[1], M. Elisa Milanesio[*], Edgardo N. Durantini[*]

Departamento de Química, Facultad de Ciencias Exactas, Físico-Químicas y Naturales, Universidad Nacional de Río Cuarto, Ruta Nacional 36 Km 601, X5804BYA Río Cuarto, Córdoba, Argentina

ARTICLE INFO

Keywords:
Phthalocyanine
Silica nanoparticles
Photodynamic activity
Microorganisms
Photoinactivation

ABSTRACT

Silica nanoparticles (SiNPs) embedded with Zn(II) 2,9,16,23-tetrakis(methoxy)phthalocyanine ($SiNPZnPcOCH_3$), Zn(II) 2,9,16,23-tetrakis(4-pyridyloxy) phthalocyanine (SiNPZnPcOPy) and Zn(II) 2,9,16,23-tetrakis(*t*-butyl) phthalocyanine (SiNPZnPctBu) were synthesized in the nonpolar core of AOT/1-butanol/water micelles using triethoxyvinylsilane and 3-aminopropyltriethoxysilane. These SiNPs-Pc presented an average diameter of about 20–25 nm. UV–vis absorption spectra presented the characteristic *Sore*t and *Q* bands of phthalocyanines embedded into the nanoparticles. Moreover, red fluorescence emission of SiNPs bearing phthalocyanines was detected in water. The SiNPs-Pc produced the photodecomposition of 2,2′-(anthracene-9,10-diyl)bis(methylmalonic acid), which was used to sense the singlet molecular oxygen $O_2(^1\Delta_g)$ generation in aqueous medium. Also, the formation of superoxide anion radical was detected by nitro blue tetrazolium reduction in the presence of NADH. Photoinactivation of microorganisms was investigated in *Staphylococcus aureus* and *Candida albicans*. *In vitro* experiments showed that photosensitized inactivation induced by $SiNPZnPcOCH_3$ and SiNPZnPctBu improved with an increase of irradiation times. After 30 min irradiation, over 7 log reduction was found for *S. aureus*. Also, these SiNPs-Pc produced a decrease of 2.5 log in *C. albicans* after 60 min irradiation. In both cases, a lower photoinactivation activity was found for SiNPZnPcOPy. Studies of photodynamic action mechanism showed that the photokilling of microbial cells was protected in the presence of sodium azide and diazabicyclo[2.2.2]octane. Also, a reduction on the cell photodamage was found with the addition of D-mannitol. Therefore, the photodynamic activity sensitized by $SiNPZnPcOCH_3$ and SiNPZnPctBu in microbial cells was mediated by a contribution of both type I and type II photooxidative mechanisms. Thus, silica nanoparticles are interesting materials to vehicle $ZnPcOCH_3$ and ZnPctBu in aqueous media to photoeradicate microorganisms.

1. Introduction

Antimicrobial resistance is a growing problem that complicates the treatment of infections acquired in the hospitals and in the community [1]. Therefore it is important to search for alternative therapeutic modalities [2]. Some modifications to the application of photodynamic therapy (PDT) for the treatment of cancer have been proposed for photokilling of microorganisms [3]. This approach, called photodynamic inactivation (PDI), is based on the preferential accumulation of the photosensitizer in the microbial cells. Subsequently, irradiation with visible light in the presence of oxygen leads to the formation of reactive oxygen species (ROS), which react with biomolecules inducing a loss of biological functionality and microbial cell inactivation [4]. Two types of photodynamic mechanisms may occur after photoactivation of photosensitizing [5]. One involves the generation of free radicals (type I) and the other the formation of singlet molecular oxygen, $O_2(^1\Delta_g)$ (type II) [6]. These highly reactive species affect the cell viability causing lethal damage in the microorganisms [7,8]. In this sense, discovery an appropriate photosensitizer is decisive in improving the efficacy of PDI. A large number of potential photosensitizers have been proposed for different microorganism [9]. In particular, phthalocyanine derivatives have been investigated as interesting photosensitizers with several biomedical applications [10,11]. This family of photosensitizers has a high molar extinction coefficient in the region of the

* Corresponding authors.
E-mail addresses: mmilanesio@exa.unrc.edu.ar (M.E. Milanesio), edurantini@exa.unrc.edu.ar (E.N. Durantini).
[1] These authors contributed equally to this work.

https://doi.org/10.1016/j.pdpdt.2018.06.020
Received 14 May 2018; Received in revised form 22 June 2018; Accepted 27 June 2018
Available online 30 June 2018

phototherapeutic window (650–800 nm), high $O_2(^1\Delta_g)$ singlet oxygen generation efficiency and high photostability [12,13]. For these reasons, the phthalocyanines have been studied mainly for their antibacterial, antifungal and antipathogenic efficacies [14,15].On the other hand, for an efficient photoinactivation effect, the phthalocyanine must be dissolved as monomers in the cell medium, because aggregate formation leads to loss of photodynamic activity [16]. However, most photosensitizers used in PDI are hydrophobic and insoluble in water. Therefore, the administration of phototherapy agents is one of the main challenges in PDI of microorganisms. In this way, the recent development of nanomedicine has opened a new front in advance in the field of phototherapy [17]. The nanoparticles, with a size ranging from 1 to 100 nm, have raised expectations for providing phototherapeutic agents to produce an effective pathological death of cells [18,19]. The versatile polymerization of silica can be used to stabilize encapsulated photosensitizers, which can maintain their properties even in photoinactivating conditions [20,21]. In particular, silica nanoparticles have been used to encapsulate several photosensitizers. SiNPs are stable to pH changes and are not subject to microbial attack. Due to the permeability of the porous matrix to molecular oxygen, ROS can be generated in the SiNPs and diffuse to kill microorganisms.

In this paper, we report the synthesis of organically modified silica-based nanoparticles embedded with phthalocyanines. Thus, SiNPs-Pc containing Zn(II) 2,9,16,23-tetrakis(methoxy)phthalocyanine ($ZnPcOCH_3$), Zn(II) 2,9,16,23-tetrakis(*t*-butyl)phthalocyanine (ZnPctBu) and Zn(II) 2,9,16,23-tetrakis(4-pyridyloxy) phthalocyanine (ZnPcOPy) were synthesized in micellar media (Fig. 1). $ZnPcOCH_3$ substituted by methoxy groups was previously evaluated as efficient phototherapeutic agent in photodynamic therapy treatments [22]. Moreover, ZnPcOPy was investigated as photosensitizer to inactivate microorganisms [13]. These phthalocyanines are non-soluble in water. Therefore, spectroscopic and photodynamic properties of SiNPs-Pc were evaluated in aqueous solution. Moreover, PDI mediated by these photosensitizers was studied in a Gram-positive bacteria *S. aureus* and a yeast *C. albicans*. To obtain insight about the mechanism of photodynamic action mediated by these SiNPs-Pc, photoinactivation was investigated in presence of different scavengers of ROS, such as sodium azide, D-mannitol and DABCO [15].

2. Materials and methods

2.1. General

Absorption and fluorescence spectra were recorded on a Shimadzu UV-2401PC spectrometer (Shimadzu Corporation, Tokyo, Japan) and on a Spex FluoroMax spectrofluorometer (Horiba Jobin Yvon Inc, Edison, NJ, USA), respectively. Fluence rates were obtained with a Radiometer Laser Mate-Q (Coherent, Santa Clara, CA, USA). Experiments of steady state photolysis in solution were carried out with a Cole-Parmer illuminator 41720-series (Cole-Parmer, Vernon Hills, IL, USA) with a 150 W halogen lamp. A wavelength range between 590 and 800 nm (14 mW/cm^2) was selected using an optical filter (OG590 cutoff filter). The visible light source used to irradiate cell suspensions was a Novamat 130 A F (Braun Photo Technik, Nürnberg, Germany) slide projector containing with a 150 W lamp. A 2.5 cm glass cuvette filled with water was used to remove the heat from the lamp. A wavelength range between 350 and 800 nm was selected by optical filters with a fluence rate of 30 mW/cm^2. Sodium bis(2-ethylhexyl)sulfosuccinate (AOT) from Sigma (St. Louis, MO, USA) was dried under vacuum. The cosurfactant 1-butanol, triethoxyvinylsilane (TEVS) and 3-aminopropyltriethoxysilane (APTES) were purchased from Aldrich (Milwaukee, WI, USA).

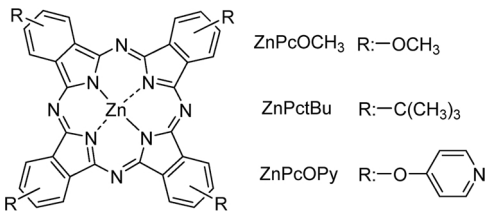

Fig. 1. Structures of phthalocyanines.

2.2. Synthesis and characterization of drug-loaded silica-based nanoparticles

ZnPcOPy, $ZnPcOCH_3$ and Zn(II)tetramethyltetrapyridino[2,3-b:2′,3′-g:2″,3″-l:2‴,3‴-q]porphyrazinium (ZnTM2,3PyPz) were synthesized as previously described [13,22,23]. ZnPctBu from Aldrich were used without further purification.

The SiNPs-Pc were synthesized in the nonpolar core of AOT/1-butanol/water micelles [24]. In a typical experiment, the micelles were prepared by dissolving 1.76 g of AOT and 3.2 mL of cosurfactant 1-butanol in 80 mL of doubly distilled water by vigorous magnetic stirring. A 500 μL sample of 15 mM phthalocyanine in *N,N*-dimetilformamida (DMF) was dissolved by magnetic stirring in the resulting clear solution. Then, triethoxyvinylsilane (800 μL) was added to the micellar system and the resulting solution was stirred for about 1 h, or until it became clear. After that, 40 μL of 3-aminopropyltriethoxysilane was added and the system stirred for about 24 h. The entire reaction was carried out at room temperature. At the end of the process, a greenish-blue translucency indicating the formation of nanoparticles was observed. After the formation of drug embedded nanoparticles, surfactant AOT and cosurfactant 1-butanol were completely removed by dialyzing the solution in water through a 12–14 kDa cutoff cellulose membrane (Spectrum Laboratories, Inc., Rancho Dominguez, CA, USA) for one week. This approach produced SiNPs-Pc, named as $SiNPZnPcOCH_3$, SiNPZnPctBu and SiNPZnPcOPy, which contain $ZnPcOCH_3$, ZnPctBu, and ZnPcOPy, respectively. Stock suspension of 2 mg nanoparticles/mL, containing 10 nmol phthalocyanine/mg nanoparticles were prepared in water. Transmission electron microscopy (TEM) was employed to determine the morphology and size of the aqueous dispersion of nanoparticles, using a transmission electron microscope Zeiss LEO 906E (Oberkochen, Germany).

2.3. Spectroscopic studies

Absorption and fluorescence spectra were recorded in a quartz cell of 1 cm path length at 25.0 ± 0.5 °C. Fluorescence emission spectra of nanoparticles were obtained in water exciting the samples at 610 nm, while the fluorescence excitation spectra were performed using a wavelength of emission at 700 nm. The fluorescence quantum yield (Φ_F) of phthalocyanines encapsulated in SiNPs were calculated by comparison of the area below the corrected emission spectrum in water with that of ZnTM2,3PyPz as a reference ($\Phi_F = 0.29$) [23]. Sample and reference absorbances were matched at the excitation wavelength (610 nm) and the areas of the emission spectra were integrated in the range 630–800 nm.

2.4. Steady state photolysis

Solutions of 2,2′-(anthracene-9,10-diyl)bis(methylmalonic acid) (ABMA, 35 μM) and nanoparticles (photosensitizer absorbance ~0.1 at $\lambda = 680$ nm for nanoparticles and 630 nm for the reference ZnTM2,3PyPz) in water (2 mL) were irradiated in a quartz cell of 1 cm path length. The kinetics of ABMA photooxidation were studied following the decrease of the fluorescence (I) at $\lambda_{max} = 428$ ($\lambda_{exc} = 378$ nm) [25]. The observed rate constants (k_{obs}) were obtained by a linear least-squares fit of the semilogarithmic plot of Ln I_0/I *vs.* time. Quantum yields of $O_2(^1\Delta_g)$ production (Φ_Δ) were calculated in water comparing the k_{obs} for the corresponding SiNPs-Pc with that for

ZnTM2,3PyPz (Φ_Δ = 0.65) [23]. ZnTM2,3PyPz was used as a reference due to its solubility in aqueous media. Measurements of the sample and reference under the same conditions afforded Φ_Δ for photosensitizers by direct comparison of the slopes in the linear region of the plots.

2.5. Detection of superoxide anion radical

The photooxidation of nitro blue tetrazolium (NBT) was used to detect superoxide anion radical ($O_2^{\cdot -}$) formation. The nitro blue tetrazolium (NBT) method was carried out using 0.2 mM NBT, 0.5 mM NADH and photosensitizer (absorbance 0.3 at *Soret* band) in 2 mL of DMF/water (9/1) [26]. Control experiments were performed in absence of NBT, NADH or photosensitizer. The progress of the reaction was monitored by following the increase of the absorbance at λ = 560 nm.

2.6. Bacterial and yeast strain and preparation of cultures

The microorganisms used in this study were the strains of *S. aureus* ATCC 25923 and *C. albicans* (PC31), which were previously characterized and identified [27,28]. Microbial cells were grown aerobically in sterile condition overnight at 37 °C in 4 mL tryptic soy or Sabouraud (Britania, Buenos Aires, Argentina) broths for cultures of bacteria or yeast, respectively. An aliquot (60 μL) of the bacterial culture was aseptically transferred to 4 mL of fresh tryptic soy broth and incubated at 37 °C to exponential phase of growth (absorbance 0.7 at 660 nm). Cells were centrifuged (3000 rpm for 15 min) and re-suspended in equal amount of 10 mM phosphate-buffered saline (PBS, pH = 7.4) solution, corresponding to ~10^8 colony forming units (CFU)/mL. After overnight cultures of *C. albicans*, cells were harvested by centrifugation (3000 rpm for 15 min) and re-suspended in PBS. Yeast cells (absorbance 0.5 at 650 nm) were diluted 1:4 in PBS to obtain ~10^6 CFU/mL. After each assay, cell suspensions were serially diluted 10-fold in PBS. Cell suspensions were quantified by the spread plate counting method in triplicate for estimating the survival rate of microorganisms. Viable microbial cells were monitored and the number of CFU was determined after ~24 h (bacteria) or ~48 h (*C. albicans*) incubation at 37 °C in the dark.

2.7. Photosensitized inactivation of microorganisms

Cells suspensions (2 mL, ~10^8 CFU/mL bacteria and ~10^6 CFU/mL yeast) in PBS were treated with the photosensitizer $SiNPZnPcOCH_3$, SiNPZnPcOPy and SiNPZnPctBu (0.01 mM). The photosensitizer was added from a stock solution (0.02 mM) in water. The cultures were incubated in the dark at 37 °C for 30 min. Then, 200 μL of each cell suspension were transferred to 96-well microtiter plates (Deltalab, Barcelona, Spain) and exposed for different time intervals with visible light. Cell viability was determined as described above.

2.8. Photoinactivation of S. aureus and C. albicans cell suspensions under different conditions

Cell suspensions of *S. aureus* (2 mL, ~10^8 CFU/mL) and *C. albicans* (2 mL, ~10^6 CFU/mL) in PBS were treated with 1 mg/mL SiNPs-Pc, which correspond to 10 μM phthalocyanine, for 30 min in dark at 37 °C. Photodynamic activity of SiNPs-Pc was studied in presence of sodium azide, diazabicyclo[2.2.2]octane (DABCO) and D-mannitol. These compounds were added from a stock solution 1 M sodium azide, 0.2 M DABCO and 2 M D-mannitol in water. The concentration of these additives in the cell suspensions were 100 mM sodium azide, 10 mM DABCO and 100 mM D-mannitol. After that, the cultures were exposed to visible light for 15 min and 60 min for bacteria and yeast, respectively. Cells were quantified as described above.

2.9. Controls and statistical analysis

Control experiments were carried out in the presence and absence of SiNPs-Pc in the dark and in the absence of SiNPs-Pc with cells irradiated. Three values were obtained per each condition and each experiment was repeated separately three times. Differences between means were tested for significance by one-way ANOVA. Results were considered statistically significant with a confidence level of 95% ($p < 0.05$). Data were represented as the mean ± standard deviation of each group.

3. Results and discussion

3.1. Synthesis of SiNPs-Pc

Phthalocyanine derivatives used in la synthesis of nanoparticles are shown in Fig. 1. These phthalocyanines are lipophilic compounds insoluble in water [13,22]. In particular, $ZnPOCH_3$ was an effective photosensitizer with applications in PDT *in vitro* and *in vivo* for the treatment of accessible malignancies [29,30]. Also, ZnPOPy and ZnPtBu are active photosensitizers in organic solvent [13]. Therefore, these phthalocyanines were chose to load SiNPs with photosensitizers. Silica-based nanocarriers embedded with phthalocyanines were synthesized in the non-polar core of AOT/1-butanol/water micelles using triethoxyvinylsilane as silica precursor [24]. This approach was performed using 15 mM of $ZnPOCH_3$, ZnPOPy and ZnPtBu to yield $SiNPZnPcOCH_3$, SiNPZnPcOPy and SiNPZnPctBu, respectively. This concentration of phthalocyanine was used to obtain an excess of photosensitizer in the reaction medium. After the formation SiNPs-Pc, these were purified by dialyzing the solution against water in order to eliminate the remaining phthalocyanine. The dialyzed solutions were stable SiNPs-Pc suspensions in water, as shown in Fig. 2. The size and shape of SiNPs-Pc bearing phthalocyanines was observed by TEM. Typical images for SiNPs-Pc are shown in Fig. 3. In the three cases, similar results were found. The silica-based nanocarriers are spherical, having uniform size distribution, with an average size of 20–25 nm. SiNPs-Pc of similar size were previously reported encapsulating photosensitizers for *in vitro* photodynamic therapy [24,31].

3.2. Spectroscopic properties of SiNPs-Pc

The UV–vis absorption spectra of the SiNPs-Pc are displayed in Fig. 4A. Spectra showed the typical *Soret* band at ~350 nm and *Q*-bands in the region between 550–750 nm. However, the bands of phthalocyanine were broader and shifted in comparison with those of monomeric phthalocyanine in DMF (Fig. 4B) [32,33]. These phthalocyanines showed an intense *Q*-band in the region of ~678 nm, which is characteristic of Zn(II)phthalocyanine derivatives dissolved as monomeric molecules in DMF [13,22]. The spectra of SiNPZnPcOPy showed two intense peaks in water (Fig. 4A), the one at 635 nm corresponds to absorption by the aggregate, while the other at 677 nm was due to

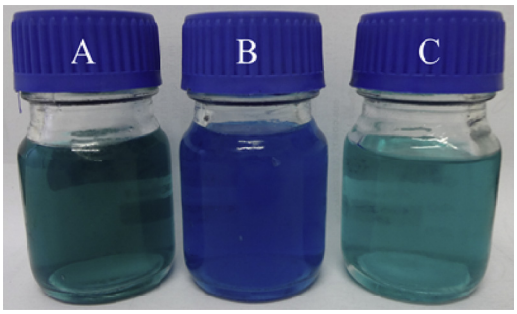

Fig. 2. Suspension of (A) $SiNPZnPcOCH_3$, (B) SiNPZnPctBu and (C) SiNPZnPcOPy in water.

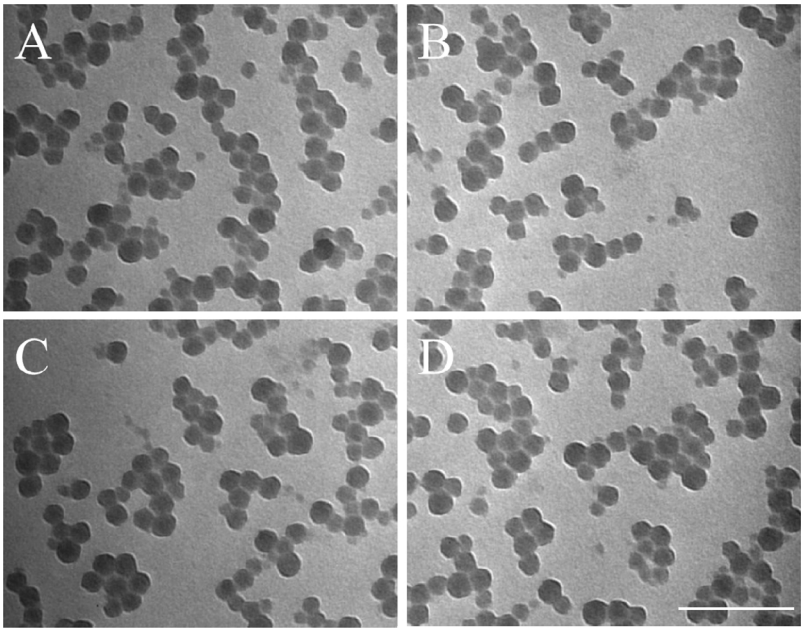

Fig. 3. TEM image of SiNPs-Pc silica-based nanocarriers (A) SiNPs, (B) SiNPZnPcOCH$_3$, (C) SiNPZnPctBu (D) SiNPZnPcOPy; scale bar 0.1 μm.

absorption by the monomeric molecule [16]. Less intense and widened absorption bands were observed for SiNPZnPcOCH3 and SiNPZnPctBu. Therefore, the absorption spectra indicated that the photosensitizers are partially aggregated in the SiNPs-Pc, mainly when the phthalocyanines ZnPcOCH3 and ZnPctBu were used.

Fig. 5 shows the fluorescence emission spectra of aqueous dispersion of SiNPZnPcOCH$_3$, SiNPZnPcOPy and SiNPZnPctBu entrapped in nanoparticles. In Fig. 5 the spectra showed the two bands in the red spectral region with a more intense peak at ~685 nm, which are typical of Zn(II)phthalocyanine [22]. Since aggregated phthalocyanines are non-emissive, the emission observed upon excitation at 610 nm occurs from the monomeric species [34]. These bands have been assigned to *Q* (0–0) and *Q*(0–1) transitions [35]. Moreover, the inset in Fig. 5 shows the excitation spectra of solutions following the nanoparticles 717 nm emission. These results indicate that maintain the form of the corresponding absorption spectra of phthalocyanines. Thus, no significant change in the peak positions of the excitation spectra were observed respect to free phthalocyanine in solution (Fig. 4B). This is because the species responsible for the emission of the SiNPs-Pc is the phthalocyanine monomer embedded in them. A small Stokes shift (5–10 nm) was observed for the phthalocyanines in the SiNPs-Pc indicating that the spectroscopic energy is nearly identical to the relaxed energy of the singlet state. That suggests that only a minor geometric relaxation occurs in the first excited state [10].

Fluorescence quantum yields (Φ_F) of these SiNPs-Pc were determined by comparing with ZnTM2,3PyPz as a reference [23]. The values of Φ_F (≤ 0.01) for the phthalocyanines incorporated into SiNPs-Pc were considerably lower than those of the same in solution [13,22]. These results are in agreement with the partial aggregation of the phthalocyanines in the SiNPs-Pc observed by UV–vis absorption spectroscopy as shown in Fig. 4A.

3.3. Singlet molecular oxygen production

Anthracene derivatives with hydrophilic substituents can serve as $O_2(^1\Delta_g)$ traps in aqueous solution [36]. Thus, the photooxidation of anthracene derivative ABMA sensitized by SiNPs-Pc embedded with Zn (II)phthalocyanines was studied in water. Under these conditions, the $O_2(^1\Delta_g)$ generated converts ABMA into its corresponding endoperoxide forms, leading to the reduction in the intensity of the peaks in its absorption spectra [25]. Typical results of first-order plots for the photooxidation of ABMA in aqueous solutions photosensitized by SiNPs-Pc are shown in Fig. 6. The values of the observed rate constant (k_{obs}) were calculated from first-order kinetic plots of the ABMA emission at 428 nm *vs.* time. As can be observed in Table 1, a higher value of k_{obs} was obtained for SiNPZnPctBu followed by SiNPZnPcPy, whereas SiNPZnPcOCH$_3$ were the least effective SiNPs-Pc to decompose ABMA. Also, the photooxidation of ABMA sensitized by SiNPs-Pc were compared with that induced by ZnTM2,3PyPz in water. It is know that this phthalocyanine represents an active photosensitizer to produce $O_2(^1\Delta_g)$ in aqueous medium because ZnTM2,3PyPz is soluble in water as monomer [23]. Thus, higher value of k_{obs} (3.46 ± 0.2) x10^{-3} s^{-1} for ABMA was obtained for the reaction photosensitized in solution by this cationic phthalocyanine. As can be observed, SiNPZnPcOCH$_3$ presents a k_{obs} value of 100 times less than the reference phthalocyanine, whereas the k_{obs} values of SiNPZnPcOPy and SiNPZnPctBu were 30 to 13 times smaller than that found for ZnTM2,3PyPz. Taking into account that ABMA quenches $O_2(^1\Delta_g)$ exclusively by chemical reaction, this substrate can be used as a method to evaluate the ability of the photosensitizers to produce $O_2(^1\Delta_g)$ in solution [37]. The quantum yield of $O_2(^1\Delta_g)$ production (Φ_Δ) were calculated comparing the k_{obs} for the corresponding phthalocyanine with that for the reference. As shown in Table 1, the SiNPs-Pc produced lower Φ_Δ than the reference [23]. Thus, increased production of $O_2(^1\Delta_g)$ was found for SiNPZnPcOPy and SiNPZnPctBu, while a lower value was for NPZnPcOCH$_3$. The decrease in the $O_2(^1\Delta_g)$ production of phthalocyanines may be due to a partial aggregation of the photosensitizer embedded in the SiNPs-Pc. It is known, that the phenomenon of aggregation decreased the photodynamic properties of photosensitizers [16].

3.4. Formation of superoxide anion radical

Generation of $O_2\cdot^-$ by SiNPs bearing phthalocyanines was evaluated using NBT reduction to diformazan in presence of NADH, following the absorption at 510 nm in water [26]. Photosensitized decomposition of NBT takes place predominantly through a type I photoreaction process [38]. The increase in diformazan absorption was investigated as a function of time after irradiation with visible light. As can be observed in Fig. 7, decomposition of NBT significantly increases in presence of SiNPs-Pc and NADH after irradiation with respect to

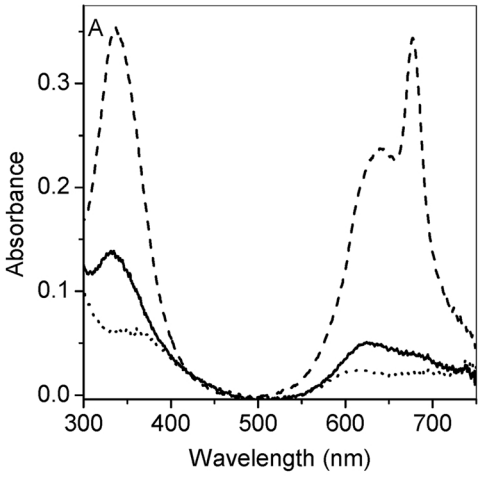

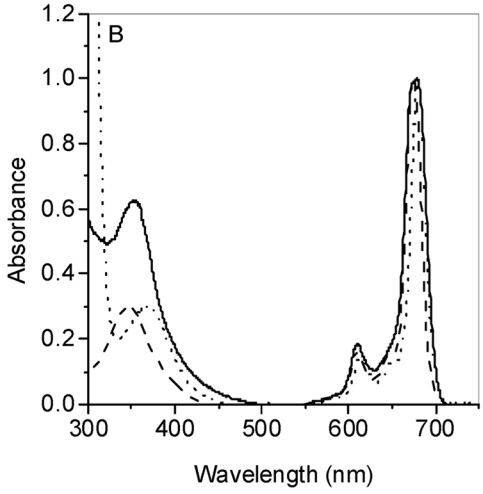

Fig. 4. Absorption spectra of (A) $SiNPZnPcOCH_3$ (solid line), SiNPZnPctBu (dashed line) and SiNPZnPcOPy (dotted line) in water and (B) $ZnPcOCH_3$ (solid line), ZnPctBu (dashed line) and ZnPcOPy (dotted line) in DMF.

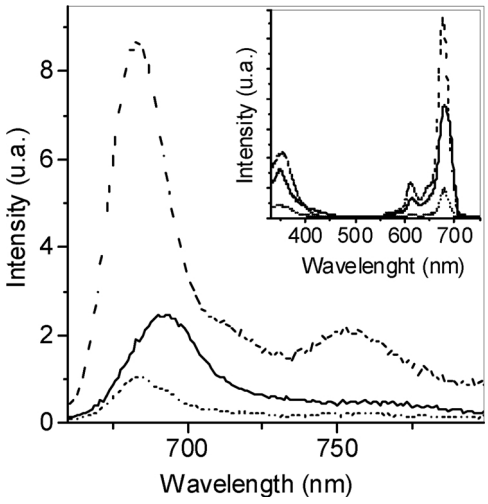

Fig. 5. Fluorescence emission spectra of nanoparticles $SiNPZnPcOCH_3$ (solid line), SiNPZnPctBu (dashed line) and SiNPZnPcOPy (dotted line) in water (λ_{exc} = 610 nm). Inset: spectra excitation of $SiNPZnPcOCH_3$ (solid line), SiNPZnPctBu (dashed line) and SiNPZnPcOPy (dotted line) in water (λ_{em} = 700 nm).

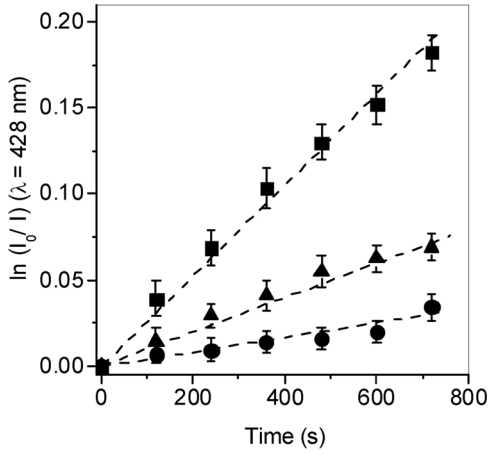

Fig. 6. First-order plots for the photooxidation of ABMA (35 μM) photosensitized by the nanoparticles $SiNPZnPcOCH_3$ (●), SiNPZnPctBu (■) and SiNPZnPcOPy (▲) in water; λ_{exc} = 378 nm, λ_{irr} = . 590–800 nm.

Table 1
Spectroscopic data, kinetic parameters (k_{obs}) for the photooxidation reaction of ABMA and quantum yield of $O_2(^1\Delta_g)$ production (Φ_Δ) of SiNPs-Pc in water.

SiNPs-Pc	λ_{max}^{abs} (nm)	λ_{max}^{em} (nm)	k_{obs}^{ABMA} (s^{-1})	Φ_Δ [a]
$SiNPZnPcOCH_3$	682	692	(3.89 ± 0.04)x10^{-5}	0.007 ± 0.001
SiNPZnPctBu	678	683	(2.66 ± 0.06)x10^{-4}	0.049 ± 0.004
SiNPZnPcOPy	677	683	(1.04 ± 0.05)x10^{-4}	0.019 ± 0.002

[a] using ZnTM2,3PyPz as a reference, k_{obs}^{ABMA} = (3.46 ± 0.05) × 10^{-3} s^{-1}, Φ_Δ = 0.65 [23].

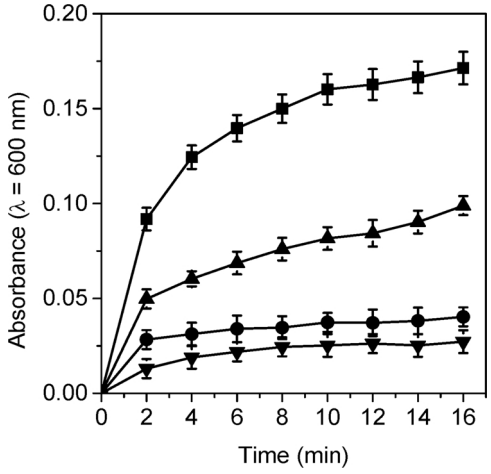

Fig. 7. Reduction of NBT (0.2 mM) sensitized by $SiNPZnPcOCH_3$ (●), SiNPZnPctBu (■) and SiNPZnPcOPy (▲) in presence NADH (0.5 mM) as an increase in the absorption at 510 nm in DMF/water (9:1). Control with NBT and NADH without photosensitizer (▼);λ_{irr} = 590–800 nm.

solution without the photosensitizers. A faster formation of diformazan was observed in presence of SiNPZnPctBu than SiNPZnPcPy, while a lower NBT decomposition was found using $SiNPZnPcOCH_3$. Therefore, even though $O_2(^1\Delta_g)$ can be generated by photoexcited triplet state of phthalocyanines, it was observed that $O_2\cdot^-$ can also be produced in the presence of NADH.

3.5. PDI of microbial cell suspensions

The photodynamic action induced by SiNPs-Pc was compared to inactivate *S. aureus* and *C. albicans* cell suspensions in PBS. Thus, *S.*

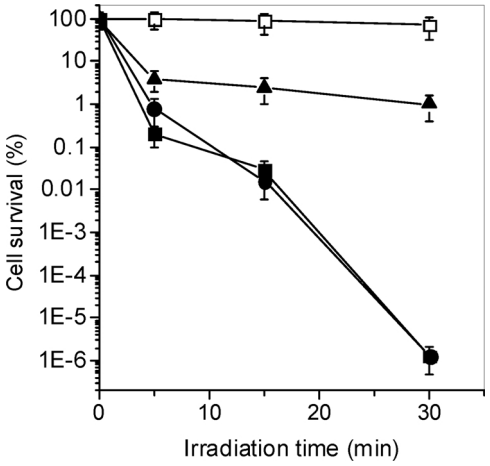

Fig. 8. Survival curves of *S. aureus* cells (~10^8 CFU/mL) incubated with nanoparticles (0.01 mM) of SiNPZnPcOCH$_3$ (●), SiNPZnPctBu (■) and SiNPZnPcOPy (▲) for 15 min at 37 °C in dark and exposed to visible light for different irradiation times. Control culture (□) corresponds to cells suspension without SiNPs-Pc and irradiated.

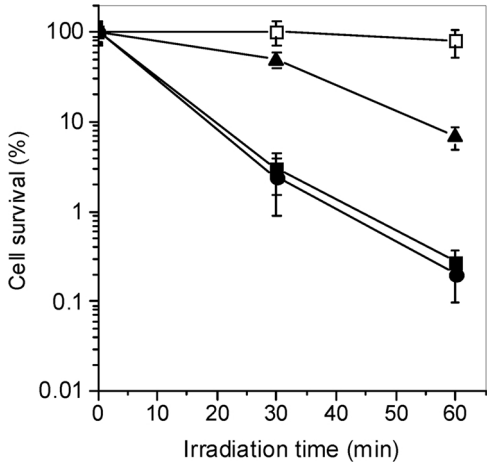

Fig. 9. Survival curves of *C. albicans* cells (~10^6 CFU/mL) incubated with nanoparticles (0.01 mM) of SiNPZnPcOCH$_3$ (●), SiNPZnPctBu (■) and SiNPZnPcOPy (▲) for 30 min at 37 °C in dark and exposed to visible light for different irradiation times. Control culture (□) corresponds to cells suspension without SiNPs-Pc and irradiated.

aureus cells were treated with (0.01 mM) of SiNPZnPcOCH$_3$, SiNPZnPcOPy and SiNPZnPctBu for 30 min at 37 °C in dark and exposed to visible light for different irradiation times (5, 15 and 30 min). The Fig. 8 shows the survival of bacterial cells after irradiation. Control experiments demonstrate that the viability of *S. aureus* were unaffected by illumination alone, by dark incubation with these SiNPs-Pc for 30 min or SiNPs-Pc without photosensitizers. Therefore, the cell inactivation observed after irradiation of the cultures treated with the photosensitizers was mediated by the photosensitization activity of the phthalocyanines in the SiNPs-Pc. The studies showed that the photodynamic action mediated by SiNPZnPcOCH$_3$ or SiNPZnPctBu produced a decrease of 3.5 log in *S. aureus* cell viability after 15 min of irradiation, which represents a 99.97% cell death. In contrast, SiNPZnPcOPy caused a small effect on the viability of the microorganism (1.5 log). Under these conditions, an enhancement in the cell inactivation sensitized by SiNPZnPcOCH$_3$ or SiNPZnPctBu was found increasing the irradiation time to 30 min. Thus, these SiNPs-Pc embedded with ZnPcOCH$_3$ or ZnPctBu induced a complete eradication of *S. aureus* (over 7 log decrease). By comparison with previous studies under similar conditions, it was found that 5,10,15,20-tetrakis(4-carboxyphenyl) porphyrin covalently linked to silica-coated magnetite nanoparticles (MNPNH-TCPP) produced a 2.5 log reduction of *S. aureus* after 30 min irradiation [39]. Also, porphyrin derivatives linked to magnetic nanoparticles were effective for photoinactivation of bacteria and phages [40,41]. On the other hand, photoexcitation of phthalocyanines covalently linked to aminopropyl silica gel produced $O_2(^1\Delta_g)$ and displayed reasonable photodynamic activity against bacteria *E. coli* [42]. Instead of the phthalocyanines, the chlorin derivative was immobilized on two commercial materials, a 3-bromopropyl-functionalized silica and a Merrifield resin [43]. These materials have high potential as photosensitizer for the inactivation of Gram negative bacteria.

Photosensitized inactivation of *C. albicans* was investigated in PBS cell suspensions incubated with photosensitizers (0.01 mM). Survival curves are shown in Fig. 9. No toxicity was found for the cells treated with these concentrations of SiNPs-Pc for 60 min in dark. Moreover, the viability of microbial cells was not affected by irradiation without photosensitizer. The results showed that the presence of SiNPZnPcOPy induced only 1 log of photokilling after 30 min irradiation. In contrast, a higher photoinactivation of cells was observed in the presence of SiNPZnPcOCH$_3$ or SiNPZnPctBu. These SiNPs-Pc produced a decrease in cell survival of 2.5 log (99.7%) after 60 min irradiation. Similar results were previously obtained for *C. albicans* treated with MNPNH-TCPP [39]. The fungal cell walls have a relatively thick layer of β-glucan and chitin that leads to permeability barrier greater than Gram-positive bacteria [44]. Thus, *S. aureus* cells were more susceptible to the photodynamic activity mediated by SiNPs-Pc, while *C. albicans* required longer irradiation or higher concentration to obtain significant eradication.

3.6. Photodynamic action mechanism induced by SiNPs-Pc in microbial cells

Mechanism studies were performed with nanoparticles SiNPZnPcOCH$_3$ and SiNPZnPctBu because they were able to inactivate *S. aureus* and *C. albicans*. Cell suspensions of *S. aureus* (~10^8 CFU/mL) were treated with 0.01 mM for 15 min in dark and then the cultures were irradiated for 15 min with visible light. On the other hand, *C. albicans* cells (~10^6 CFU/mL) were incubated with 2 mg/mL for 30 min in dark and irradiated for 60 min. These conditions were chosen because they allowed observing either possible protective effects or an increase in the inactivation of cells. The simplest approach for determining whether $O_2(^1\Delta_g)$ and/or ROS are involved in a photodynamic inactivation process is to study the SiNPs-Pc efficacy in the presence of various $O_2(^1\Delta_g)$ quenchers and ROS scavengers. Thus, the microorganism inactivation studies were carried out in the presence of scavengers of ROS species. Azide anion was used as a quencher of $O_2(^1\Delta_g)$ [45]. However, it also can deactivate photosensitizers in their triplet excited state preventing both type I and type II photoprocesses. Also, DABCO was used to inhibit $O_2(^1\Delta_g)$-mediated oxidations. A charge transfer-induced mechanism was suggested for the quenching of $O_2(^1\Delta_g)$ by DABCO [46]. In contrast, D-mannitol can be used as a scavenger of the superoxide anion radical ($O_2^{\cdot -}$) and hydroxyl radical (type I reaction) [47]. The $O_2(^1\Delta_g)$ quenchers sodium azide and DABCO were used at concentrations of 100 mM and 10 mM, respectively. The free radical scavenger D-mannitol was 100 mM. Control tests confirm that the viability of *S. aureus* or *C. albicans* are not affected either by irradiation itself or by any of the SiNPs-Pc tested in the dark, nor by the quenchers or scavengers tested, both in the dark or when exposed to light.

The results for *S. aureus* are shown in Figs. 10 and 11 for cells treated with SiNPZnPcOCH$_3$ and SiNPZnPctBu, respectively. In the presence of sodium azide, a reduction in PDI of 1.5 log and 3.5 log units were observed for *S. aureus* with SiNPZnPcOCH$_3$ and SiNPZnPctBu, respectively. This inhibition was in accordance with the ability of these SiNPs-Pc to generate $O_2(^1\Delta_g)$. The bacterial protection mediated by sodium azide was more evident with SiNPZnPctBu, which showed a

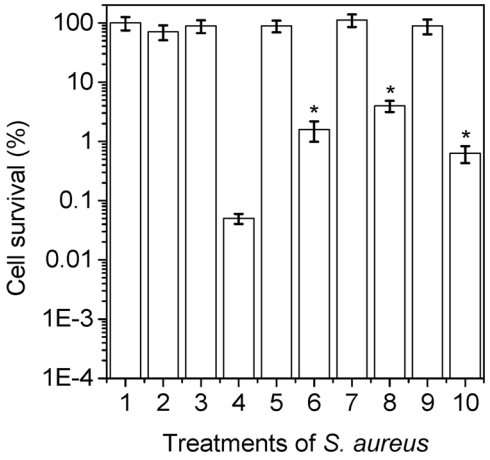

Fig. 10. Survival of *S. aureus* cells ($\sim 10^8$ CFU/mL) incubated with 0.01 mM $SiNPZnPcOCH_3$ in dark for 15 min at 37 °C and exposed to visible light for 15 min, 1) cells in dark, 2) irradiated cells, 3) cells treated with $SiNPZnPcOCH_3$ in dark, 4) irradiated cells treated with $SiNPZnPcOCH_3$, 5) cells treated with $SiNPZnPcOCH_3$ containing 100 mM azide in dark, 6) irradiated cells treated with $SiNPZnPcOCH_3$ containing 100 mM azide, 7) cells treated with $SiNPZnPcOCH_3$ containing 10 mM DABCO in dark, 8) irradiated cells treated with $NPZnPcOCH_3$ containing 10 mM DABCO, 9) cells treated with $SiNPZnPcOCH_3$ containing 100 mM D-mannitol in dark, 10) irradiated cells treated with $SiNPZnPcOCH_3$ containing 100 mM D-mannitol (*$p < 0.05$, compared with column 4).

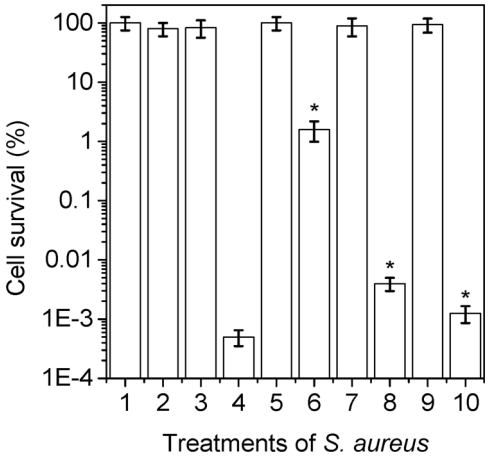

Fig. 11. Survival of *S. aureus* cells ($\sim 10^8$ CFU/mL) incubated with 0.01 mM SiNPZnPctBu in dark for 15 min at 37 °C and exposed to visible light for 15 min, 1) cells in dark, 2) irradiated cells, 3) cells treated with SiNPZnPctBu in dark, 4) irradiated cells treated with SiNPZnPctBu, 5) cells treated with SiNPZnPctBu containing 100 mM azide in dark, 6) irradiated cells treated with SiNPZnPctBu containing 100 mM azide, 7) cells treated with SiNPZnPctBu containing 10 mM DABCO in dark, 8) irradiated cells treated with SiNPZnPctBu containing 10 mM DABCO, 9) cells treated with SiNPZnPctBu containing 100 mM D-mannitol in dark, 10) irradiated cells treated with SiNPZnPctBu containing 100 mM D-mannitol (*$p < 0.05$, compared with column 4).

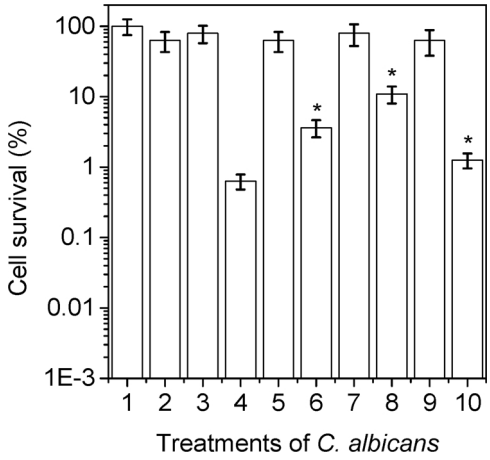

Fig. 12. Survival of *C. albicans* cells ($\sim 10^6$ CFU/mL) incubated with 1 mM $SiNPZnPcOCH_3$ in dark for 30 min at 37 °C and exposed to visible light for 60 min, 1) cells in dark, 2) irradiated cells, 3) cells treated with $SiNPZnPcOCH_3$ in dark, 4) irradiated cells treated with $SiNPZnPcOCH_3$, 5) cells treated with $SiNPZnPcOCH_3$ containing 100 mM azide in dark, 6) irradiated cells treated with $SiNPZnPcOCH_3$ containing 100 mM azide, 7) cells treated with $SiNPZnPcOCH_3$ containing 10 mM DABCO in dark, 8) irradiated cells treated with $SiNPZnPcOCH_3$ containing 10 mM DABCO, 9) cells treated with $SiNPZnPcOCH_3$ containing 100 mM D-mannitol in dark, 10) irradiated cells treated with $SiNPZnPcOCH_3$ containing 100 mM D-mannitol (*$p < 0.05$, compared with column 4).

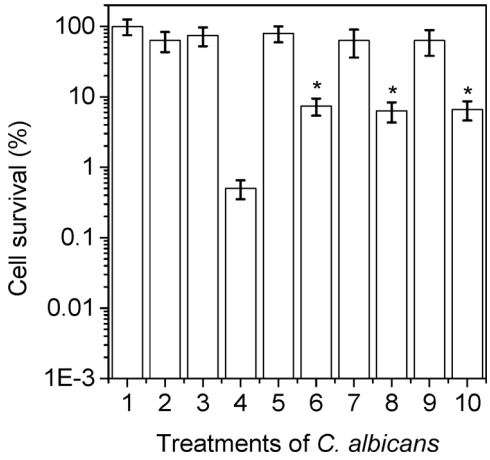

Fig. 13. Survival of *C. albicans* cells ($\sim 10^6$ CFU/mL) incubated with 0.01 mM SiNPZnPctBu in dark for 30 min at 37 °C and exposed to visible light for 60 min, 1) cells in dark, 2) irradiated cells, 3) cells treated with SiNPZnPctBu in dark, 4) irradiated cells treated with SiNPZnPctBu, 5) cells treated with SiNPZnPctBu containing 100 mM azide in dark, 6) irradiated cells treated with SiNPZnPctBu containing 100 mM azide, 7) cells treated with SiNPZnPctBu containing 10 mM DABCO in dark, 8) irradiated cells treated with SiNPZnPctBu containing 10 mM DABCO, 9) cells treated with SiNPZnPctBu containing 100 mM D-mannitol in dark, 10) irradiated cells treated with SiNPZnPctBu containing 100 mM D-mannitol (*$p < 0.05$, compared with column 4).

higher $O_2(^1\Delta_g)$ production. The addition of DABCO produced a 2 log in *S. aureus* photoinactivation treated with $SiNPZnPcOCH_3$, while it was about 1 log in presence of SiNPZnPctBu. Also, a 1 log decrease in *S. aureus* photokilling was observed in presence of D-mannitol with $SiNPZnPcOCH_3$, while a lower effect (0.4 log) was found using SiNPZnPctBu. On the other hand, the effects of these ROS scavengers in *C. albicans* cells are shown in Figs. 12 and 13 for $SiNPZnPcOCH_3$ and SiNPZnPctBu, respectively. The results indicate that in the presence of $SiNPZnPcOCH_3$ photoinactivation was mainly protected in presence of azide ions (0.8 log) and DABCO (1.2 log), while a slight effect was found with D-mannitol (0.3 log). When SiNPZnPctBu was used as photosensitizer, a reduction of 1 log in C. albicans photoinactivation was obtained for the three scavengers.

After activation of the phthalocyanines embedded in the SiNPs two oxidative mechanisms can mainly take place, which are considered to be principally implicated in the cell photodamage [5]. In the type I photoprocess, the photosensitizer interacts with substrates to yield free radicals. The majority of these radicals instantaneously reacts with oxygen and generates a complicated mixture of highly ROS. In contrast, $O_2(^1\Delta_g)$ is produced in the type II mechanism as the main species

responsible for cell inactivation. These intermediates are capable to oxidize a wide variety of biomolecules leading to a loss of appropriate biological functionality [3]. The production of $O_2(^1\Delta_g)$ sensitized by $SiNPZnPcOCH_3$ and SiNPZnPctBu was detected in water. Moreover, the formation of $O_2^{\cdot -}$ through a type I photoreaction process mediated by these SiNPs-Pc was observed in aqueous solutions. Thus, dependent on experimental conditions, both $O_2(^1\Delta_g)$ and $O_2^{\cdot -}$ must be involved in the photodynamic activity. Furthermore, even if an excited photosensitizer reacts with a given substrate by type I photoprocess, the final result is also the oxidation of essential biomolecules. In a biological medium, both mechanisms can occur simultaneously and the ratio between the two processes is influenced by the photosensitizer, substrates and the nature of the environment. It was previously observed that the killing of *C. albicans* cells by zinc(II) 2,9,16,23-tetrakis [4-(*N*-methylpyridyloxy)]phthalocyanine and visible light irradiation seem to be mediated mainly by $O_2(^1\Delta_g)$ [15]. The studies of PDI sensitized by $SiNPZnPcOCH_3$ and SiNPZnPctBu indicate a contribution of type I and type II photooxidative mechanisms, although the photokilling of *S. aureus* by SiNPZnPctBu and *C. albicans* by $SiNPZnPcOCH_3$ showed a lower influence of type I pathway.

4. Conclusions

In this study, SiNPs embedded with $ZnPcOCH_3$, ZnPctBu or ZnPcOPy phthalocyanines were prepared with an average diameter of about 20–25 nm. The Soret and Q-bands absorptions indicated that these phthalocyanines were partially aggregated in the SiNPs-Pc. Moreover, the characteristic red fluorescence emission of phthalocyanines was observed in water. These SiNPs-Pc were able to produce $O_2(^1\Delta_g)$ and $O_2^{\cdot -}$ in presence of NADH in aqueous medium. *In vitro* experiments showed that $SiNPZnPcOCH_3$ and SiNPZnPctBu were effective photosensitizers to eradicate *S. aureus* and *C. albicans*. The results of this study showed that $O_2(^1\Delta_g)$ mediated reactions (type II mechanism) represent the main pathway through which the $SiNPZnPcOCH_3$ and SiNPZnPctBu exert their photodynamic action. However, the data obtained also support that free radicals-mediated reactions occur and contribute to photoinactivation, but in a much smaller extension in the case of $SiNPZnPcOCH_3$ on *S. aureus* and in the case of SiNPZnPctBu on *C. albicans*.

Acknowledgments

Authors are grateful to Consejo Nacional de Investigaciones Científicas y Técnicas (CONICET, PIP-2015 1122015 0100197 CO) of Argentina, Universidad Nacional de Río Cuarto (UNRC-SECYT PPI-2016 18/C460) and Agencia Nacional de Promoción Científica y Tecnológica (ANPCYT, PICT 0667/16) of Argentina for financial support. M.G.A., M.E.M. and E.N.D. are Scientific Members of CONICET. E.B. and E.R. thank to CONICET for the research fellowships.

References

[1] M. Frieri, K. Kumar, A. Boutin, Antibiotic resistance, J. Infect. Public Health 10 (2017) 369–378.
[2] A. Nigama, D. Gupta, A. Sharma, Treatment of infectious disease: beyond antibiotics, Microbiol. Res. 169 (2014) 643–651.
[3] N. Kashef, M.R. Hamblin, Can microbial cells develop resistance to oxidative stress in antimicrobial photodynamic inactivation? Drug Resist. Update 31 (2017) 31–42.
[4] A.M. Durantini, D.A. Heredia, J.E. Durantini, E.N. Durantini, BODIPYs to the rescue: potential applications in photodynamic inactivation, Eur. J. Med. Chem. 144 (2018) 651–661.
[5] E. Alves, M.A. Faustino, M.G. Neves, A. Cunha, J. Tome, A. Almeida, An insight on bacterial cellular targets of photodynamic inactivation, Future Med. Chem. 6 (2014) 141–164.
[6] T. Dai, B.B. Fuchs, J.J. Coleman, R.A. Prates, C. Astrakas, T.G.St. Denis, M.S. Ribeiro, E. Mylonakis, M.R. Hamblin, G.P. Tegos, Concepts and principles of photodynamic therapy as an alternative antifungal discovery platform, Front. Microbiol. 3 (2012) 1–16.
[7] E.N. Durantini, Photodynamic inactivation of bacteria, Curr. Bioact. Compd. 2 (2006) 127–142.
[8] F. Pereira Gonzales, T. Maisch, Photodynamic inactivation for controlling *Candida albicans* infection, Fungal Biol. 116 (2012) 1–10.
[9] A. Martinez De Pinillos Bayona, P. Mroz, C. Thunshelle, M.R. Hamblin, Design features for optimization of tetrapyrrole macrocycles as antimicrobial and anticancer photosensitizers, Chem. Biol. Drug Des. 89 (2017) 192–206.
[10] A.L. Ochoa, T.C. Tempesti, M.B. Spesia, M.E. Milanesio, E.N. Durantini, Synthesis and photodynamic properties of adamantylethoxy Zn(II) phthalocyanine derivatives in different media and in human red blood cells, Eur. J. Med. Chem. 50 (2012) 280–287.
[11] M.A. Di Palma, M.G. Alvarez, A.L. Ochoa, M.E. Milanesio, E.N. Durantini, Optimization of cellular uptake of zinc(II) 2,9,16,23-tetrakis[4-(*N*-methylpyridyloxy)]phthalocyanine for maximal photoinactivation of Candida albicans, Fungal Biol. 117 (2013) 744–751.
[12] T. Nyokong, Effects of substituents on the photochemical and photophysical properties of main group metal phthalocyanines, Coord. Chem. Rev. 251 (2007) 1707–1722.
[13] I. Scalise, E.N. Durantini, Synthesis, properties, and photodynamic inactivation of Escherichia coli using a cationic and noncharged Zn(II) pyridyloxyphthalocyanine derivatives, Bioorg. Med. Chem. 13 (2005) 3037–3045.
[14] M. Ke, J.M. Eastel, K.L.K. Ngai, Y. Cheung, P.K.S. Chan, M. Hui, D.K.P. Ng, P. Lo, Photodynamic inactivation of bacteria and viruses using two monosubstituted zinc (II) phthalocyanines, Eur. J. Med. Chem. 84 (2014) 278–283.
[15] M.A. Di Palma, M.G. Alvarez, E.N. Durantini, Photodynamic action mechanism mediated by zinc(II) 2,9,16,23-tetrakis [4-(*N*-methylpyridyloxy)]phthalocyanine in *Candida albicans* cells, Photochem. Photobiol. 91 (2015) 1203–1209.
[16] M.P. Cormick, M. Rovera, E.N. Durantini, Synthesis, spectroscopic properties and photodynamic activity of a novel Zn(II) phthalocyanine substituted by fluconazole groups, J. Photochem. Photobiol. A: Chem. 194 (2008) 220–229.
[17] M. Karimi, A. Ghasemi, P.S. Zangabad, R. Rahighi, S.M.M. Basri, H. Mirshekari, M. Amiri, Z. Shafaei Pishabad, A. Aslani, M. Bozorgomid, D. Ghosh, A. Beyzavi, A. Vaseghi, A.R. Aref, L. Haghani, S. Bahrami, M.R. Hamblin, Smart micro/nanoparticles in stimulus-responsive drug/gene delivery systems, Chem. Soc. Rev. 45 (2016) 1457–1501.
[18] M. Veerapandian, K. Yun, Functionalization of biomolecules on nanoparticles: specialized for antibacterial applications, Appl. Microbiol. Biotechnol. 90 (2011) 1655–1667.
[19] S.S. Lucky, K.C. Soo, Y. Zhang, Nanoparticles in photodynamic therapy, Chem. Rev. 115 (2015) 1990–2042.
[20] E. Thienot, M. Germain, K. Piejos, V. Simon, A. Darmon, J. Marill, E. Borghi, L. Levy, J.-F. Hochepied, A. Pottier, One pot synthesis of new hybrid versatile nanocarrier exhibiting efficient stability in biological environment for use in photodynamic therapy, J. Photochem. Photobiol. B: Biol. 100 (2010) 1–9.
[21] N. Kashef, Y.-Y. Huang, M.R. Hamblin, Advances in antimicrobial photodynamic inactivation at the nanoscale, Nanophotonics 6 (2017) 853–879.
[22] E.I. Yslas, V. Rivarola, E.N. Durantini, Synthesis and photodynamic activity of zinc (II) phthalocyanine derivatives bearing methoxy and trifluoromethylbenzyloxy substituents in homogeneous and biological media, Bioorg. Med. Chem. 13 (2005) 39–46.
[23] T.C. Tempesti, J.C. Stockert, E.N. Durantini, Photosensitization ability of a water soluble zinc(II)tetramethyltetrapyridinoporphyrazinium salt in aqueous solution and biomimetic reverse micelles medium, J. Phys. Chem. B 112 (2008) 15701–15707.
[24] I. Roy, T.Y. Ohulchanskyy, H.E. Pudavar, E.J. Bergey, A.R. Oseroff, J. Morgan, T.J. Dougherty, P.N. Prasad, Ceramic-based nanoparticles entrapping water-insoluble photosensitizing anticancer drugs: a novel drug-carrier system for photodynamic therapy, J. Am. Chem. Soc. 125 (2003) 7860–7865.
[25] S.J. Mora, M.E. Milanesio, E.N. Durantini, Spectroscopic and photodynamic properties of 5,10,15,20-tetrakis[4-(3-N,N-dimethylaminopropoxy)phenyl]porphyrin and its tetracationic derivative in different media, J. Photochem. Photobiol. A: Chem. 270 (2013) 75–84.
[26] D.D. Ferreyra, E. Reynoso, P. Cordero, M.B. Spesia, M.G. Alvarez, M.E. Milanesio, E.N. Durantini, Synthesis and properties of 5,10,15,20-tetrakis[4-(3-N,N-dimethylaminopropoxy)phenyl] chlorin as potential broad-spectrum antimicrobial photosensitizers, J. Photochem. Photobiol. B: Biol. 158 (2016) 243–251.
[27] M.B. Spesia, M. Rovera, E.N. Durantini, Photodynamic inactivation of Escherichia coli and Streptococcus mitis by cationic zinc(II) phthalocyanines in media with blood derivatives, Eur. J. Med. Chem. 47 (2010) 2198–2205.
[28] M.P. Cormick, M.G. Alvarez, M. Rovera, E.N. Durantini, Photodynamic inactivation of Candida albicans sensitized by tri- and tetra-cationic porphyrin derivatives, Eur. J. Med. Chem. 44 (2009) 1592–1599.
[29] E.I. Yslas, E.N. Durantini, V.A. Rivarola, Zinc-(II) 2,9,16,23-tetrakis (methoxy) phthalocyanine: potential photosensitizer for use in photodynamic therapy in vitro, Bioorg. Med. Chem. 15 (2007) 4651–4660.
[30] E.I. Yslas, C. Prucca, S. Romaninia, E.N. Durantini, M. Bertuzzia, V. Rivarola, Biodistribution and phototherapeutic properties of Zinc (II) 2,9,16,23-tetrakis (methoxy) phthalocyanine in vivo, Photodiagn. Photodyn. Ther. 6 (2009) 62–70.
[31] C. Mauriello Jimenez, Y. Galàn Rubio, V. Saunier, D. Warther, V. Stojanovic, L. Raehm, C. Frochot, P. Arnoux, M. Garcia, A. Morère, N. Bettache, M. Maynadier, P. Maillard, M. Gary-Bobo, J.-O. Durand, 20-nm-sized mesoporous silica nanoparticles with porphyrin photosensitizers for in vitro photodynamic therapy, J. Sol-Gel Sci. Technol. 79 (2016) 447–456.
[32] M. Kostka, P. Zimcik, M. Miletin, P. Klemera, K. Kopecky, Z. Musil, Comparison of aggregation properties and photodynamic activity of phthalocyanines and azaphthalocyanines, J. Photochem. Photobiol. A: Chem. 178 (2006) 16–25.
[33] S. Wei, J. Zhou, D. Huang, X. Wang, B. Zhang, J. Shen, Syntesis and typeI/type II photosensitizing properties of a novel amphiphilic zinc phthalocyanine, Dyes Pigm.

71 (2006) 61–67.
[34] M. Kostka, P. Zimcik, M. Miletin, P. Klemera, K. Kopecky, Z. Musil, Comparison of aggregation properties and photodynamic activity of phthalocyanines and azaphthalocyanines, J. Photochem. Photobiol. A: Chem. 178 (2006) 16–25.
[35] A. Ogunsipe, D. Maree, T. Nyokong, Solvent effect on the photochemical and fluorescence properties of zinc phthalocyanine derivatives, J. Mol. Struct. 650 (2003) 131–140.
[36] G.R. Martinez, F. Garcia, L.H. Catalani, J. Cadet, M.C.B. Oliveira, G.E. Ronsein, S. Miyamoto, M.H.G. Medeiros, P. Di Mascio, Synthesis of a hydrophilic and non-ionic anthracene derivative, the N,N´-di-(2,3-dihydroxypropyl)-9,10-anthracenedipropanamide as a chemical trap for singlet molecular oxygen detection in biological systems, Tetrahedron 62 (2006) 10762–10770.
[37] M.G. Alvarez, M.L. Gómez, S.J. Mora, M.E. Milanesio, E.N. Durantini, Photodynamic inactivation of Candida albicans using bridged polysilsesquioxane films doped with porphyrin, Bioorg. Med. Chem. 20 (2012) 4032–4039.
[38] Y. Yamakoshi, N. Umezawa, A. Ryu, K. Arakane, N. Miyata, Y. Goda, T. Masumizu, T. Nagano, Active oxygen species generated from photoexcited fullerene (C_{60}) as potential medicines: $O_2^{-}\cdot$ versus $^1O_2$, J. Am. Chem. Soc. 125 (2003) 12803–12809.
[39] A.C. Scanone, N.S. Gsponer, M.G. Alvarez, E.N. Durantini, Photodynamic properties and photoinactivation of microorganisms mediated by 5,10,15,20-tetrakis(4-carboxyphenyl)porphyrin covalently linked to silica-coated magnetite nanoparticles, J. Photochem. Photobiol. A: Chem. 346 (2017) 452–461.
[40] C.M.B. Carvalho, E. Alves, L. Costa, J.P.C. Tomé, M.A.F. Faustino, M.G.P.M.S. Neves, A.C. Tomé, J.A.S. Cavaleiro, A. Almeida, A. Cunha, Z. Lin, J. Rocha, Functional cationic nanomagnet-porphyrin hybrids for the photoinactivation of microorganisms, ACS Nano 4 (2010) 7133–7140.
[41] E. Alves, J.M.M. Rodrigues, M.A.F. Faustino, M.G.P.M.S. Neves, J.A.S. Cavaleiro, Z. Lin, A. Cunha, M.H. Nadais, J.P.C. Tomé, A. Almeida, A new insight on nanomagnet-porphyrin hybrids for photodynamic inactivation of microorganisms, Dyes Pigm. 110 (2014) 80–88.
[42] N.A. Kuznetsova, O.A. Yuzhakovaa, M.G. Strakhovskayab, A.O. Shumarinab, A.S. Kozlovc, A.A. Krasnovskyc, O.L. Kaliyaa, New heterogeneous photosensitizers with phthalocyanine molecules covalently linked to aminopropyl silica gel, J. Porphyr. Phthalocyan. 15 (2011) 718–726.
[43] M.Q. Mesquita, J.C.J.M.D.S. Menezes, S.M.G. Piresa, M.G.P.M.S. Neves, M.M.Q. Simões, A.C. Tomé, J.A.S. Cavaleiro, Â. Cunha, A.L. D-da-Silva, A. Almeida, M.A.F. Faustino, Pyrrolidine-fused chlorin photosensitizer immobilized on solid supports for the photoinactivation of Gram negative bacteria, Dyes Pigm. 110 (2014) 123–133.
[44] G. Morace, F. Perdoni, E. Borghi, Antifungal drug resistance in Candida species, J. Glob. Antimicrob. Resist. 2 (2014) 254–259.
[45] E.F.F. da Silva, B.W. Pedersen, T. Breitenbach, R. Toftegaard, M.K. Kuimova, L.G. Arnaut, P.R. Ogilby, Irradiation- and sensitizer-dependent changes in the lifetime of intracellular singlet oxygen produced in a photosensitized process, J. Phys. Chem. B 116 (2012) 445–461.
[46] C. Schweitzer, R. Schmidt, Physical mechanisms of generation and deactivation of singlet oxygen, Chem. Rev. 103 (2003) 1685–1757.
[47] T. Maisch, C. Bosl, R.-M. Szeimies, N. Lehn, C. Abels, Photodynamic effects of novel XF porphyrin derivatives on prokaryotic and eukaryotic cells, Antimicrob. Agents Chemother. 49 (2005) 1542–1552.